İstanbul Journal of Pharmacy,
IJP 2025, 55 (3): 352–365

https://doi.org/10.26650/IstanbulJPharm.2025.1677873
Submitted: 17.04.2025
Revision Requested: 08.07.2025
Last Revision Received: 01.09.2025
Accepted: 01.10.2025

İstanbul Journal of Pharmacy

Research Article

Open Access

Design and Optimisation of a Biosurfactant-Synthetic Surfactant Hybrid Nanoemulgel Containing Lemon Balm and Star Anise Essential Oils: Stability, Cytotoxicity, and Antiviral Activity Against HSV-1

Tuğba Kaman [1,2], Ebru Altuntaş [3] ✉, Zakaria Ouzaid [1,3], Merve Yılmaz [3], Hasan Sercan Palancı [4], Mustafa Altındiş [5] & Sibel Yavru [4]

[1] İstanbul University, Graduate School of Health Sciences, İstanbul, Türkiye
[2] Üsküdar University, Vocational School of Health Services, Medical and Aromatic Plants, İstanbul, Türkiye
[3] İstanbul University, Faculty of Pharmacy, Department of Pharmaceutical Technology, Istanbul, Türkiye
[4] Selcuk University, Department of Virology, Faculty of Veterinary Medicine, Konya, Türkiye
[5] Sakarya University, Department of Basic Medical Sciences, School of Medicine, Sakarya, Türkiye

Abstract

Background and Aims: *Herpes simplex* virus type 1 (HSV-1) is a widespread herpetic pathogen responsible for recurring mucocutaneous infections that are frequently debilitating and difficult to treat. The objective of this work was to design and study the efficiency of a biosurfactant–synthetic surfactant hybrid nanoemulgel (NEG) system with antiviral activity against HSV-1 using *Melissa officinalis* and *Illicium verum* essential oils.

Methods: Nanoemulsions (NEs) were prepared through ultrasonic emulsification and stabilised using *Quillaja saponaria* saponins and Kolliphor® P 188. Selected NEs were mixed into xanthan gum-based gels to create NEGs. The formulations were assessed for their physicochemical properties, rheological behaviour, and stability. The CCK-8 assay was employed to evaluate the *in vitro* cytotoxicity on Vero cells. The antiviral activity against HSV-1 was assessed by measuring the tissue culture infectious dose 50% ($TCID_{50}$) values.

Results: Optimized NEGs demonstrated stable nano-sized droplets, a negative zeta potential, shear-thinning rheology, and preserved structural integrity throughout a 3-month storage duration. Both test (T) and placebo (P) formulations demonstrated dose-dependent cytotoxicity; however, T exhibited marginally lower cytotoxicity across all dilutions. Antiviral studies demonstrated that T significantly decreased the HSV-1 titre by 17.78-fold at a 1/2000 dilution compared with the untreated control, whereas P resulted in only a 1.77-fold reduction, thereby confirming the role of essential oils in antiviral efficacy.

Conclusion: The developed NEG incorporating essential oils from *Melissa officinalis* and *Illicium verum* demonstrated notable antiviral activity against HSV-1, along with satisfactory cytocompatibility. The results indicate its potential effectiveness as a topical antiviral treatment for managing HSV-1 infections.

Keywords Antiviral Activity · Essential Oils · Herpes Simplex Virus · *Melissa officinalis* · Nanoemulgel · Star Anise

Citation: Kaman, T., Altuntaş, E., Ouzaid, Z., Yılmaz, M., Palancı, H. S., Altındiş, M. & Yavru, S. (2025). Design and optimisation of a biosurfactant-synthetic surfactant hybrid nanoemulgel containing lemon balm and star anise essential oils: Stability, cytotoxicity, and antiviral activity against HSV-1. *İstanbul Journal of Pharmacy*, *55*(3), 352-365. https://doi.org/10.26650/IstanbulJPharm.2025.1677873

This work is licensed under Creative Commons Attribution-NonCommercial 4.0 International License.
© 2025. Kaman, T., Altuntaş, E., Ouzaid, Z., Yılmaz, M., Palancı, H. S., Altındiş, M. & Yavru, S.

✉ Corresponding author: Ebru Altuntaş ebru.altuntas@istanbul.edu.tr

INTRODUCTION

Herpes simplex virus (HSV) infections are recognised as a significant global public health issue (van de Sand et al., 2021). Herpes labialis, the most common viral skin infection, is induced by herpes simplex virus 1 (HSV-1), resulting in various asymptomatic or symptomatic mucocutaneous lesions referred to as cold sores or fever blisters (Leung & Barankin, 2017).

The disease is contagious and, depending on the prominent visibility of the lesion, can cause significant discomfort or pain, affecting the quality of life and leading to embarrassment and psychological distress (Sivesind et al., 2022). Infection, especially in immunocompromised patients, is serious and progressive and leads to morbidity and mortality (Zhang et al., 2019).

Although many vaccine candidates have been investigated in clinical trials, there is no licenced vaccine for preventing HSV infections. In recent years, numerous antiviral agents aimed at viral DNA polymerase have received approval for the management of acute HSV infections. Currently recognised antiviral medications for HSV include acyclovir, valacyclovir, famciclovir, cidofovir, and foscarnet (Jiang et al., 2016). The pharmacological efficacy of these drugs mainly depends on their ability to inhibit the virus-specific enzymes thymidine kinase and DNA polymerase. Some antiviral therapies may cause adverse side effects, and the development of virus strains resistant to commonly used anti-herpesvirus drugs is an increasing concern, particularly for immunocompromised patients (Schnitzler et al., 2001). Therefore, there is an immediate necessity to identify new antiviral agents to combat HSV infections (Allahverdiyev et al., 2004).

The pharmaceutical industry is increasingly targeting medicinal plants to identify lead compounds, with a particular focus on suitable alternative antiviral agents. Antiviral medicinal plants show antiviral activity with different mechanisms of action in the fight against many viruses that cause serious epidemics that pose significant risks to human health (Demir & Akpinar, 2021; Zhang et al., 2019). Studies have shown that plant phytochemicals are involved in the direct treatment process of viral infections and play a role in supportive treatment (Allahverdiyev et al., 2004).

Essential oils and their constituents are also known to be active against various microorganisms. Phenylpropanoids and sesquiterpenes in essential oils contribute to their antiviral activity. *Melissa officinalis* is a herb that is often favoured for treating cold sores because it is effective in fighting viruses in the herpes virus family. It can be used to prevent the spread of viral infections, which can be particularly useful for people who develop resistance to commonly used antiviral agents (Astani et al., 2014).

Rosmarinic acid, the primary phenolic compound in Melissa essential oil, is reported to be a key component in the virucidal effect, significantly inhibiting herpesviral binding and attachment. It can be used as a topical treatment for HSV infections and herpes viruses, regardless of their sensitivity or resistance to acyclovir (Astani et al., 2012).

Star anise essential oil demonstrated anti-HSV-1 properties by neutralising free viral particles in laboratory suspensions. In the tests, the trans-ethanol-rich star anise oil showed a selectivity index of 160 against HSV, whereas among its isolated components, only β-caryophyllene exhibited a selectivity index of 140. While acyclovir suppresses viral replication by targeting DNA polymerase within the cell, star anise oil, along with phenylpropanoids and sesquiterpenes, is believed to deactivate HSV before it enters the host cell (Astani et al., 2011).

In topical treatments, the skin functions as a principal protective barrier, identifying active pharmaceutical ingredients (APIs) as exogenous substances and restricting their absorption into the body. The stratum corneum, the outermost layer of the epidermis, serves as the primary and most resilient barrier that must be traversed for a medicine to permeate the skin effectively (Szumała & Macierzanka, 2022).

Nanocarriers have been identified as a promising approach for overcoming the stratum corneum barrier while minimising skin damage and enhancing drug penetration (KC et al., 2021; Pandi et al., 2018; Saka et al., 2020). Among these advanced delivery systems, NEs stand out due to their high drug-loading capacity, excellent solubilisation ability, ease of production, stability, and controlled release properties. Because of their lipophilic core, NEs facilitate the transport of lipophilic molecules across topical membranes more effectively than liposomes (Nafisi & Maibach, 2017). These systems exhibit excellent thermodynamic stability, contributing to a longer shelf-life than conventional emulsions, micelles, or suspensions. However, despite their many advantages, NEs have the disadvantage of low viscosity. This can result in a reduced retention time and limited spreadability (Shukla et al., 2018). These problems can be solved by the modification of NEs into a nanoemulgel (NEG) using a suitable gelling agent (Nastiti et al., 2017).

Considering the above information, this study aimed to develop a NEG formulation containing lemon balm essential oil and star anise essential oil for topical application on HSV-1. In this context, NEs were first prepared using the ultrasonic emulsification method. When choosing the ingredients for the

formulation, both biological and functional factors were considered. Saponins from *Quillaja saponaria* were employed as natural biosurfactants because of their superior emulsifying properties and known antiviral effects. To ensure the stability of the formulation and manage the droplet size, Kolliphor® P188 (poloxamer 188) was selected. Transcutol® HP (diethylene glycol monoethyl ether) was added to serve as a co-surfactant and to boost penetration. Xanthan gum was incorporated into the NE to create a NEG, enhancing the product's viscosity, spreadability, and retention on the skin. DL-α-tocopherol acetate was included as an antioxidant to prevent the degradation of oils. Sensiva™ PA 30 and caprylic/capric triglyceride were chosen to improve the stabilisation of the oil phase and to increase the dermal tolerability.

Parameters such as droplet size, polydispersity index (PdI), and zeta potential were evaluated on the prepared NE formulations before and after the accelerated stability tests (thermal test and centrifuge test), and the most suitable formulations were mixed in a natural polymeric gel containing xanthan gum at certain ratios and brought into the NEG form. After the characterisation of the prepared NEGs by various methods, accelerated stability tests (thermal test and centrifuge test) and physicochemical stability tests for 3 months were carried out on the selected formulations. Finally, *in vitro* cytotoxicity and antiviral activity tests of the optimised NEG formulation were carried out and the potential effects of the use of the developed nanotechnological formulation on herpes were investigated.

MATERIALS AND METHODS

Materials

Transcutol® HP was purchased from Gattefossé, France. Caprylic/Capric Triglyceride was obtained from Croda, Türkiye. Sensiva™ PA 30 was from Ashland, Türkiye. Lemon balm (*Melissa officinalis*) essential oil and Star Anise (*Illicium verum*) essential oil were kindly gifted by Doalinn, Türkiye. Vanzan® NF-C was kindly supplied by Vanderbilt Minerals, USA. *Quillaia saponaria molina extract* (Q-Naturale® 200 V) was kindly gifted by Ingredion GmbH, Germany. DL-alpha tocopherol acetate and Kolliphor® P 188 were obtained from Sigma- Aldrich, Germany. All other chemicals were of analytical grade.

Preparation of the Nanoemulsions

Oil phase-to-Smix ratios of 1:1.5, 1:2, and 1:3 were used to formulate NEs with an oil phase at three different concentrations (5%, 7.5%, and 10% w/w). Q-Naturale® 200 V (7.5% w/w) and Kolliphor® P 188 (5% w/w) were utilised as surfactants, whereas Transcutol® HP (2.5% w/w) functioned as a co-surfactant.

The formulations were obtained through the ultrasonic emulsification method. Initially, the ingredients of the aqueous and oily phases were accurately weighed in two separate beakers. Then, to prepare the NEs, the aqueous phase was directly added to the oil phase, followed by ultrasonication at varying durations (5, 10, or 15 min). The procedure was conducted using a 20 kHz Sonicator (Ultrasonics, USA) with a maximum power output of 750 W, configured at 50% amplitude, employing a pulse cycle of 30 s on and 30 s off.

To avoid overheating, the temperature of the mixture was maintained during the ultrasonication process by positioning the sample beaker within an ice-filled container. The formulation's composition and manufacturing parameters are detailed in Table 1. Finally, the prepared NEs were characterised, and accelerated stability studies were conducted.

Table 1. Components and production procedures of the NEs.

	Ingredients	FORMULATIONS		
	(% w/w)	F1 (P1-P3)	F2 (P1-P3)	F3 (P1-P3)
OIL PHASE	Lemon balm essential oil	0.9	0.9	0.9
	Star anise essential oil	0.9	0.9	0.9
	DL-alpha tocopherol acetate	0.2	0.2	0.2
	Caprylic/capric triglyceride	1	3.5	6
	Sensiva® PA 30	2	2	2
	Transcutol® HP	2.5	2.5	2.5
AQUEOUS PHASE	Kolliphor® P 188	5	5	5
	Q-Naturale® 200 V	7.5	7.5	7.5
	Distilled Water (d.w.)	80	77.5	75
PROCEDURES PROCESS	**Procedure 1 (P1):** 5-min ultrasound emulsification **Procedure 2 (P2):** 10-min ultrasound emulsification **Procedure 3 (P3):** 15 min ultrasound emulsification			

Preparation of the Nanoemulgels

According to the procedure reported in the literature, the NEGs were obtained with slight modifications (Mulia et al., 2018). Briefly, the selected NEs containing melissa and star anise essential oils were incorporated into polymeric gel bases at varying xanthan gum concentrations (1%, 1.5%, and 2% w/w) to formulate the NEGs. The NEs were mixed with the gel base at three different weight ratios (1:1, 1:2 or 1:3) using a magnetic stirrer at 500 rpm for 10 min to obtain the final NEGs. The formulations were then left undisturbed for 24 h to eliminate any trapped air bubbles.

Formulation Characterisation

Mean droplet size, PdI, and zeta potential analysis

The mean droplet size, PdI, and zeta potential of the formulations were determined using dynamic light scattering with a Zetasizer Nano ZS (Malvern Instruments, Ltd., Malvern, UK) (Ozkan et al., 2022). To minimise multiple scattering effects, the samples were first diluted (1:100) with distilled water. Subsequently, 2 mL of each diluted sample was placed into single-use polystyrene cuvettes. Measurements were performed within 24 h of sample preparation at 25 °C. The mean droplet size was determined using photon correlation spectroscopy, which evaluates the variations in the scattered light caused by the Brownian motion of the droplets. The zeta potential was measured through laser Doppler anemometry by applying an electric field to the samples. To ensure the reliability of the results, all measurements were performed in triplicate.

Electrical Conductivity and pH Measurements

The electrical conductivity of the formulations was directly measured using a portable conductivity metre (Hanna Edge, USA). The pH measurement was conducted by immersing the electrode of the pH metre (Hanna Edge, USA) directly in the samples. All measurements were conducted in triplicate at 25 ± 2 °C (Kildaci et al., 2021).

Rheological Properties

The viscosity of the NEGs (cP) was assessed at various shear rates with a Brookfield cone and plate viscometer (Brookfield Engineering Laboratories, Inc., Middleboro, MA, spindle no: CP-40) without prior dilution. Measurements were performed at a constant temperature of 25 ± 0.5 °C. The viscosity data of the NEs were plotted versus the shear rate to study their rheological behaviour (Dalo et al., 2022).

Accelerated Stability Studies

NEs are colloidal dispersions defined by their tiny droplet sizes and thermodynamic instability, requiring thorough stability evaluations to guarantee their effectiveness and longevity. Two frequently used techniques (centrifugation and thermal stress testing) were performed to assess the physical stability of NEs and NEGs (Ozkan et al., 2022).

Centrifugation test: A sample of NEs or NEGs weighing 5 g was subjected to centrifugation at 3500 rpm for 30 min using a laboratory centrifuge (Nüve Cooling Centrifuge, Turkey) to expedite the assessment of potential instability issues.

Thermal stress test: A thermal stress test was conducted on both NE and NEG formulations. Glass tubes with 5 g of sample were subjected to temperatures between 40 °C and 80 °C, in 5 °C increments, for 30 min at each temperature using a thermostatic water bath (Witeg WSB-30, Germany).

Physicochemical Stability Studies

To assess the physicochemical stability of the selected NEGs, freshly manufactured samples were maintained in closed glass vials at three temperatures for three months: 25 ± 2 °C and 60% RH, 40 ± 2°C and 75% RH, and 5 ± 3 °C. Samples were analyzed for mean droplet size, PdI, zeta potential, viscosity, pH, and conductivity at specified time intervals. All experiments were conducted in triplicate (Dalo et al., 2022).

Texture Profile Analysis (TPA)

The texture profile analyses of the selected NEGs were evaluated using a CT3 Texture Analyser (Brookfield, UK) to determine the mechanical parameters such as hardness, compressibility, adhesion, and cohesion. A 12.7-cm-diameter analytical probe was immersed twice in each sample between the end of the first compression and the beginning of the second, with a defined recovery time (15 s), to a defined depth (10 mm), at a defined speed (2 mm/s), and a trigger force of 0.01 N was applied. Three replicate analyses of each sample were performed. Data acquisition and calculation were performed using TexturePro CT V1.6 Build. From the resulting force-time graphs, hardness (the force required to achieve a given deformation), compressibility (the work required to deform the product during the first pass of the probe), adhesion (the work required to overcome the attractive forces between the surface of the sample and the surface of the probe) and cohesion (the ratio of the area under the force-time curve produced in the second compression cycle to that produced in the first compression cycle) were obtained (Altuntaş & Yener, 2017).

In Vitro Cell Culture Studies

Cell Cultures and Viruses

The *in vitro* cytotoxicity and antiviral activity studies were conducted at the Virology Department Laboratory, Faculty of Veterinary Medicine, Selçuk University. In this study, in the propagation of the viruses and in the concentration dose experiments, the infectious potency and antiviral activity were determined. For these *in vitro* experiments, African green monkey kidney cell culture and HSV-1 Kos strain were obtained from the Cell Culture and Virus Collection Bank at the Virology Department, Faculty of Veterinary Medicine, Selçuk University.

The cultivation of Vero cells and the viral replication process were performed using F-12 Ham/Dulbecco's Modified Eagle's Medium (DMEM, Gibco) at 37 °C in a 5% CO_2 incubator. For cell culture, the medium was supplemented with 10% foetal bovine serum (FBS), 1% antibiotic (5,000 U/mL, Gibco),

and 1% L-glutamine (200 mM, Gibco). During viral replication, a modified medium containing 2% FBS, 1% antibiotic (5,000 U/mL), and 1% L-glutamine (200 mM) was used.

Microscopic Evaluation of Nanoemulgels on Vero Cell Culture and Dose-Dependent Effects on Cell Viability

For this purpose, a 12-well cell culture plate was used for each of the F1P2-coded NEG containing 1% xanthan gum (designated as T) and the placebo NEG (designated as P). The P formulation was prepared using the same excipients (*Quillaja saponaria* saponins, Kolliphor® P188, Transcutol® HP, xanthan gum, DL-α-tocopherol acetate, caprylic/capric triglyceride, Sensiva® PA 30, and water) without the addition of essential oils. Thus, the P group represented the effect of the formulation ingredients alone, while the T group contained the essential oils in addition to the base formulation.

Each well was seeded with 500 µL of a Vero cell suspension at a density of 4.5 × 10^5 cells/mL, prepared from pre-subcultured Vero cell lines. To allow the cells to reach the exponential growth phase, the plates were incubated at 37 °C with 5% CO_2 for 24 h. Once the cells formed an approximately 80% confluent monolayer, the cell culture medium was removed. The tested formulations (T and P) were diluted in maintenance medium containing 2% FBS at ratios of 1/500, 1/750, 1/1000, 1/1500, and 1/2000. For each dilution, 500 µL was added to two replicate wells. The remaining two wells served as the untreated cell control group, receiving only 500-µL the maintenance medium containing 2% FBS. After treatment, the plates were incubated at 37 °C with 5% CO_2 for 48 h. Daily microscopic observations were conducted to assess the effects of the NEG dilutions on the cells.

Cytotoxicity Test

Vero cells were seeded in 96-well plates at a density of 5 × 10^3 – 1 × 10^4 cells per well and incubated at 37 °C with 5% CO_2 for 24 h to allow attachment. The culture medium was then replaced with 100 µL of fresh medium containing the test compounds at various dilution ratios (1/500, 1/750, 1/1000, 1/1500, 1/1750 and 1/2000). The control groups included untreated cells (negative control) and blank wells (medium only). Following a 48-h incubation at 37 °C with 5% CO_2, 10 µL of CCK-8 reagent was added to each well, and the plates were incubated for an additional 1 h.

At the end of the incubation period, the plates were analysed using a microplate reader (Tecan Infinite F50) set to measure the optical density (OD) at 450 nm, with the background absorbance at 650 nm. The results were evaluated in terms of the inhibition concentration (IC). Each test was performed in triplicate for each compound. The arithmetic mean of the obtained values from the wells was calculated, and cytotoxicity curves were generated using CurveExpert Professional software. The results were calculated using the following formula:

$$IC\% = \frac{[(ODcontrol - ODcontrol\ blank) - (OD\ Sample - OD\ Sample\ Blank)]}{(ODcontrol - ODcontrol\ blank)} \times 100$$

Antiviral Activity Studies

The antiviral activity of the T and P formulations against HSV-1 was determined by calculating the 50% endpoint titre (TCID50) of HSV-1, following the method described by Frey and Liess (1971) (Frey & Liess, 1971). The antiviral activities of the formulations were assessed separately in 96-well plates. Vero cells were prepared at a density of 8.0 × 10^5 cells/mL, and a cell suspension was prepared for this purpose. From this suspension, 100 µL was added to each well, and the plates were incubated at 37 °C with 5% CO_2 overnight to allow the cells to reach the exponential growth phase. Once the cells covered approximately 90% of the well surface as a monolayer, the culture medium was removed.

The 96-well plate was divided into two sections: one containing antiviral agents (T and P formulations) and the other without. The wells in the antiviral agent section were labelled from 1 to 10, and 100 µL of the cell suspension containing the formulations at a 1/2000 dilution was added to the first four rows. The remaining section of the plate, which contained no antiviral agents, received 100 µL of the cell culture medium. To allow potential intracellular activity (i.e., blockage of virus replication), the plate was incubated for 4 h at 37 °C with 5% CO_2.

Before the end of the incubation period, to account for any potential extracellular activity of the formulations that could disrupt the viral envelope and glycoproteins involved in adsorption, HSV-1 suspensions were further manipulated. The HSV-1 suspensions for the T and P formulation groups were serially diluted (Log10 scale from 10^{-1} to 10^{-10}) in the cell culture medium containing each formulation at a 1/2000 dilution. The HSV-1 suspensions for the control wells were similarly diluted but only in the cell culture medium without formulation. All diluted virus suspensions were incubated for 30 min at 37 °C with 5% CO_2.

At the end of the incubation period, the culture medium and test substances were removed from the wells, and 100 µL of each pre-diluted HSV-1 suspension was added to the respective wells, including the control and formulation-treated wells, up to the 10th dilution step. After transferring

the virus suspensions, the plates were returned to the 37 °C, 5% CO_2 incubator.

The cytotoxic effects (CPE) of the HSV-1 inoculation on the cells in the T- and P-treated wells were monitored daily using a tissue culture microscope. CPEs were also observed in control wells inoculated with HSV-1 dilutions without any treatment. The test was terminated after 72 h, and TCID50 for HSV-1 in the wells treated with the T and P formulations was calculated using the method described by Frey and Liess (1971) (Frey & Liess, 1971).

The experimental layout is illustrated in Figure 1.

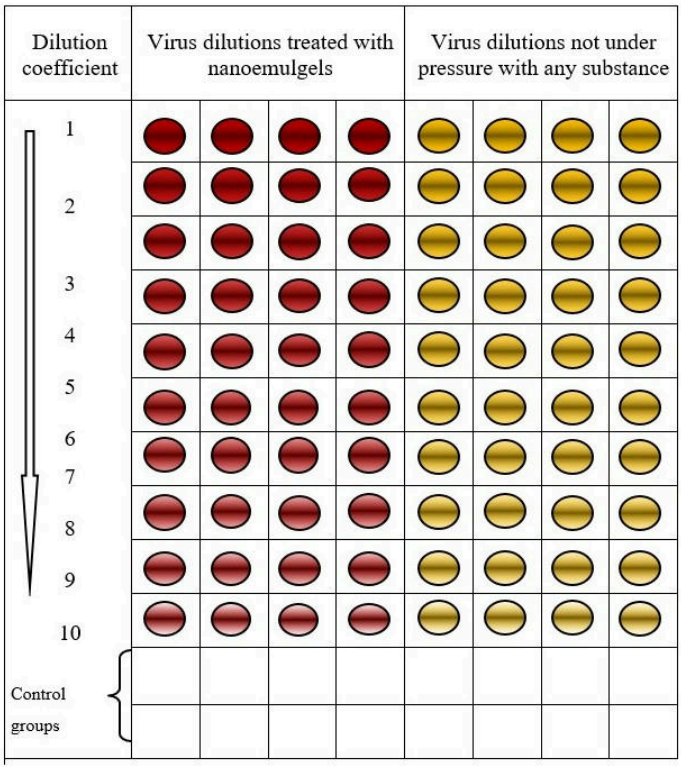

Figure 1. 96-well cell culture plate study plan

RESULTS AND DISCUSSION

Optimization and Characterization Studies

The integration of biosurfactants into NE formulations has attracted considerable interest owing to their biocompatibility, emulsification efficiency, and environmental sustainability (Banerjee et al., 2021; Yang et al., 2013). The present research, for the first time, utilised Q-Naturale® 200 V, a saponin-based biosurfactant from *Quillaja saponaria*, in combination with synthetic surfactants (Transcutol® HP and Kolliphor® P 188) to create a stable NE system. We developed our formulation strategy by integrating natural saponins with synthetic surfactants to potentially leverage the advantages of both components. This method is in accordance with recent studies that support the use of natural surfactants to improve the biocompatibility and sustainability of NEs (Doost et al., 2019; Kaur et al., 2016).

Quillaja saponaria saponins have potential advantages for treating HSV-1 because of their pharmacological activities as well as their high emulsification capacity. A study on the antiviral efficacy of aqueous extracts from *Quillaja saponaria* revealed that they can damage viral envelopes and capsid proteins, thereby lowering viral infectivity (Roner et al., 2007). The extracts exhibited broad-spectrum antiviral action, including against enveloped viruses such as HSV-1. Disruption of the viral envelope hinders the virus from attaching to and entering the host cells, reducing its infectivity. Furthermore, *Quillaja saponaria* saponins may target viral capsid proteins, thus limiting replication. Given that HSV-1 primarily affects mucosal and skin tissue, *the antiviral capabilities of Quillaja saponaria* make it a suitable topical treatment option. Furthermore, its anti-inflammatory properties may help regulate the inflammation associated with HSV infections (Sarkhel, 2016).

This study proposes that using *Quillaja saponaria* saponins alongside essential oils derived from *Melissa officinalis* (lemon balm) and *Illicium verum* (star anise) may be beneficial for the development of antiviral treatment for HSV-1. Integrating these essential oils with Quillaja saponins may increase their bioavailability and effectiveness. The surfactant properties of the saponins might strengthen the interaction of the essential oil constituents with the viral particles or host cells. In addition, the ability of saponins to form stable emulsions enhances the controlled release and extended action of essential oils.

The NEs were prepared in this study with different ratios of the oil phase to Smix, i.e., 1:1.5, 1:2 and 1:3 respectively, and oil phase concentration in 5%, 7.5% and 10% w/w. Q-Naturale® 200 V (7.5% w/w), biosurfactant; Kolliphor® P 188 (5% w/w), synthetic surfactant and Transcutol® HP (2.5% w/w), cosurfactant were used as the oil phase. The ultrasonic emulsification method was used to produce the NEs as it produces stable NEs with desired droplet sizes (Carpenter & Saharan, 2017).

The use of ultrasonic emulsification is in line with the recent literature that reported that this technique is very effective in controlling the droplet sizes and their distribution, thus enhancing the encapsulation of active ingredients and their bioavailability (Leong et al., 2009). The period of ultrasonication was modified to evaluate its influence on the droplet size, where 5, 10, and 15 min of sonication were selected according to previous literature, which suggested the ideal reduction in size while ensuring desirable stability (Nirmala et al., 2020).

During this study, an investigation was conducted into the mean droplet sizes of the prepared NEs. Based on the findings, it was ascertained that for the formulation with a low oil phase content (5% w/w), an ultrasonication duration of 10 min was optimal, yielding a NE with a mean droplet size of 168.2 ± 0.80 nm (Table 2). Conversely, for formulations with higher oil phase concentrations (7.5% and 10% w/w), an increase in ultrasonication time resulted in larger droplet sizes. Specifically, a 5-min ultrasonication duration was found to be optimal, with the smallest droplet size (162.3 ± 1.00 nm) observed in the NE containing 10% oil phase (Table 2). This observation is consistent with the findings reported in the previous literature, where the effect of the ultrasonication time on the droplet size varied with the oil phase concentration. Studies indicate that sonication typically reduces the droplet size by enhancing both the shear forces and the cavitation effects. However, when sonication is conducted for an extended duration at high oil phase levels, droplet coalescence occurs, resulting in an overall increase in size. For instance, a research indicated that an increase in sonication duration initially reduced the droplet size. Prolonged sonication beyond a specific threshold resulted in droplet coalescence, which was attributed to increased collisions among smaller droplets. This confirms that excessive energy input can destabilise the emulsion system (Gaikwad & Pandit, 2008). Similarly, it was reported that an optimal sonication time is required to balance the reduction in droplet size and prevent instability due to excessive energy input (Belgheisi et al., 2021). These observations highlight the importance of optimizing sonication parameters based on the oil phase content to achieve the desired droplet size and NE stability.

Table 2. Characterisation results of the NEs before and after the accelerated stability tests (n = 3).

Code	Mean droplet size (nm)			PdI			Zeta Potential (mV)		
	T0	ACT	ATT	T0	ACT	ATT	T0	ACT	ATT
F1P1	297.2	270.7	278.3	0.299	0.267	0.205	−43.8	−43.6	−42.0
F1P2	168.2	169.1	189.5	0.123	0.143	0.122	−39.7	−38.4	−40.2
F1P3	226.6	228.8	238.0	0.190	0.203	0.151	−43.8	−42.1	−43.7
F2P1	175.4	189.1	225.1	0.198	0.194	0.157	−39.7	−39.7	−44.6
F2P2	200.5	211.9	290.2	0.186	0.195	0.244	−41.7	−38.1	−45.8
F2P3	225.5	224.3	311.4	0.199	0.209	0.259	−41.8	−41.5	−44.2
F3P1	162.3	167.0	193.0	0.141	0.160	0.056	−38.3	−38.3	−41.3
F3P2	263.3	246.9	276.5	0.205	0.225	0.193	−41.3	−44.1	−46.3
F3P3	245.1	242.0	278.2	0.205	0.201	0.184	−42.6	−40.0	−45.0

*T0: before the accelerated stability tests; *ACT: after the centrifuge test; *ATT: after the thermal test

Despite the slight changes observed in the mean droplet size, PdI, and zeta potential after the accelerated stability tests, the formulations largely retained their NE characteristics (Table 2). Across all formulations, the droplet size remained below 500 nm, even after the thermal stress test. Although some formulations exhibited an increase in the droplet size (e.g., F2P2: 200.5 nm to 290.2 nm, F2P3: 225.5 nm to 311.4 nm), these values were still well within the nanometre range, indicating that no significant coalescence or phase separation occurred.

The PdI values remained below 0.3 in all formulations, demonstrating that the NEs maintained a narrow size distribution with relatively uniform droplet sizes. Even after thermal stress, the PdI values remained within acceptable limits, ensuring that the formulations did not undergo excessive droplet aggregation or phase separation.

Although minor variations were noted in the mean droplet size, PdI, and zeta potential following the accelerated stability tests, the formulations mostly maintained their NE characteristics (Table 2). All formulations exhibited a droplet size consistently below 500 nm, even following the thermal stress test. Even though the droplet size increased in several formulations (F2P2: 200.5 nm to 290.2 nm, F2P3: 225.5 nm to 311.4 nm), these values were still well within the nanometre range, suggesting that there was no obvious phase separation or coalescence.

The PdI values consistently remained below 0.3 across all formulations, indicating that the NEs exhibited a narrow size distribution with relatively uniform droplet sizes. After thermal stress, the PdI values were maintained within acceptable ranges, indicating that the formulations did not undergo notable droplet aggregation or phase separation.

The formulations demonstrated significant negative zeta potential values, varying from −38.3 mV to −46.3 mV, both before and following the stability testing. The values demonstrate significant electrostatic repulsion between the droplets, which aids in preventing aggregation and maintaining the long-term stability of the NEs. The substantial negative charge of *Quillaja saponaria* saponins plays a critical role in the increased negative zeta potential values seen in NE droplets, thus improving their stability (Schreiner et al., 2020). The effect primarily results from the molecular structure of saponins, characterized by hydrophilic regions containing acidic groups such as glucuronic acid, gypsogenic acid, and quillaic acid. The acidic moieties impart a negative charge to the saponin molecules, resulting in a negatively charged droplet interface upon adsorption onto the surface of the oil droplets in NEs. The presence of a negative charge generates electrostatic

repulsion between the droplets, which prevents aggregation and improves the colloidal stability.

The results indicated that the NEs preserved their structural integrity and stability, making them suitable for further application and development.

The incorporation of essential oils into NEGs can considerably enhance their skin penetration and therapeutic effects, rendering them promising candidates for topical applications. The anti-inflammatory properties of NEGs containing essential oils are emphasised in a comprehensive review by Yap et al., 2024 (Yap et al., 2024). For example, clove essential oil-loaded NEG demonstrated a higher level of efficacy in reducing inflammation symptoms than its pure form, indicating that it has the potential to be used to treat cutaneous inflammatory disorders (Aman et al., 2020).

In our study, we developed NEGs containing lemon balm essential oil and star anise essential oil to harness the advantages of NEGs for topical application. Optimizing xanthan gum concentration and the ratio of NE to the gel base is essential for developing stable NEGs. Xanthan gum enhances the rheological properties and structural integrity of the gel; however, excessive quantities may result in larger droplet sizes, elevated PdI values, and diminished stability. Consequently, precise formulation is essential to equilibrate these factors and attain NEGs with optimal performance attributes.

Among the developed NEs, F1P2 and F3P1 were selected for NEG preparation because they exhibited the smallest droplet sizes and the lowest PdI values both before and after the accelerated stability tests. In this regard, the selected NEs were incorporated into polymeric gel bases containing xanthan gum at different concentrations (1%, 1.5%, and 2% w/w) to develop the NEGs. To evaluate the effect of the gel composition, the NEs were combined with the gel base in three different weight ratios (1:1, 1:2, and 1:3). The findings demonstrated that an increase in the gel base ratio resulted in a significant

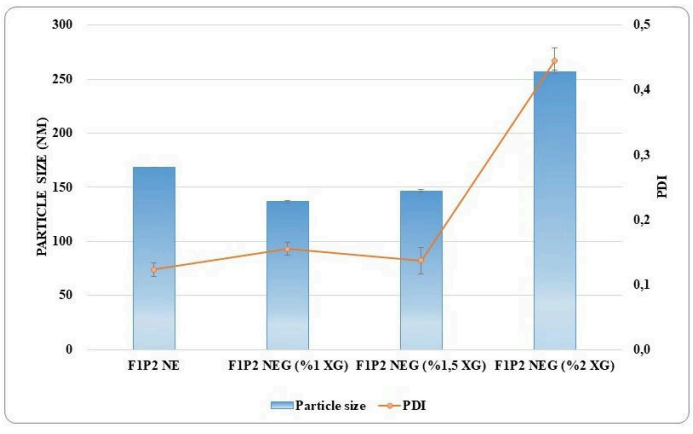

Figure 2. Effect of gelling on the mean droplet size and PdI of F1P2 coded NEs (means ± SD, n = 3). XG- Xanthan gum

enlargement of the mean droplet size and an increase in the PdI of the formulations F1P2 and F3P1. However, when these NEs were combined with the gel base in a 1:1 weight ratio, where xanthan gum was utilised at concentrations of 1% and 1.5%, the mean droplet size remained smaller compared to the unmodified NEs, despite a slight increase in the PdI values. In contrast, increasing the gel base concentration to 2% resulted in negative effects, causing an undesirable rise in both the mean droplet size and PdI (Figure 2 and Figure 3).

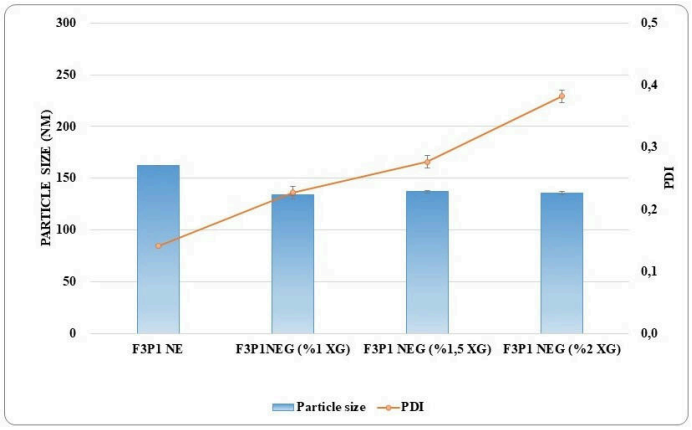

Figure 3. Effect of gelling on the mean droplet size and PdI of F3P1 coded NEs (means ± SD, n = 3). XG Xanthan- gum

The findings indicate that xanthan gum improves the structural integrity of NEGs; however, high concentrations may cause destabilisation, likely due to increased viscosity and restricted droplet mobility. The evaluation of NEGs prior to and following accelerated stability testing revealed that formulations with a 1:1 NE-to-gel base ratio and reduced xanthan gum concentrations (1% and 1.5%) demonstrated enhanced stability. The formulations preserved their nanoscale droplet size distribution and exhibited enhanced resistance to physicochemical destabilisation, highlighting the necessity of optimising the gel matrix composition for stable NEG formulations.

Based on the findings from the accelerated stability studies, the formulations coded F1P2 and F3P1, which were manufactured with a 1:1 ratio of NE to the gel base and included lower concentrations of xanthan gum (1% and 1.5%, respectively), exhibited enhanced stability profiles. Consequently, the four chosen NEG formulations underwent comprehensive testing on stability across the three-month period to evaluate their performance under storage conditions. During this storage period, a specific set of intervals was targeted for evaluation regarding the presence of any physicochemical alterations. The parameters included the organoleptic properties, mean droplet diameter, PdI, zeta potential, viscosity, pH, and electrical conductivity. The data acquired offered insights into the long-term stability and robustness of the chosen

formulations, which is essential for predicting their shelf life while ensuring consistent product quality.

According to the results, no macroscopic instability phenomena were observed in the organoleptic control, as all tested NEGs maintained their initial homogeneous and milky appearance. The droplet size and PdI values of the four selected NEG formulations remained relatively stable over the 3-month storage period under controlled conditions of 25 ± 2 °C and 60% RH, as well as 5 ± 3 °C. Under these conditions, only minimal fluctuations were observed, indicating good physical stability. In contrast, samples stored at 40 ± 2 °C and 75% RH exhibited a slight increase in both droplet size and PdI, suggesting that elevated temperature and humidity may accelerate minor destabilisation processes such as droplet aggregation or coalescence.

Among the studied formulations, F1P2 with xanthan gum 1% showed the most stable droplet properties. On day 0, F1P2 had a mean droplet size and a PdI of 132.35 nm and 0.203, respectively. After 3 months, the samples stored at 5 °C showed a further decrease in the droplet size to 114.75 nm and a PdI of 0.172, while the samples kept at 25 °C and 60% RH showed maintained values of 129.15 nm and 0.184, respectively. Under accelerated conditions (40 °C, 75% RH), the droplet size increased to 172.35 nm and the corresponding PdI was 0.207.

The maximum average droplet size for all formulations and storage conditions was 285.18 nm with a PdI of 0.290. It is noteworthy that all formulations maintained their nano-range droplet size and narrow size distribution under both stress conditions, which shows good colloidal stability and low risk of phase separation or severe aggregation. This proves that the NEG formulations are stable over time, physically confirming their suitability for further development.

The zeta potential is one of the most important parameters for determining the colloidal stability of NE-based systems, as it indicates the extent of the electrostatic repulsion between the dispersed droplets. As a general guideline, values lower or above ±30 mV are regarded as sufficient for electrostatic stabilisation (Kildaci et al., 2021). Throughout the 3 months of storage, all four NEG formulations showed zeta potential values of approximately −50 mV or lower under all tested storage conditions, which denotes excellent long-term colloidal stability.

A tendency was noted with increasing xanthan gum concentration from 1% to 1.5%, where a more negative zeta potential was observed for all formulations. This implies that xanthan gum not only contributes to the viscosity but also increases the zeta potential, most likely because of its polyanionic character giving rise to the surface charge density over the droplets.

Throughout the storage period, no significant loss of zeta potential was observed, even under accelerated conditions. For the most stable formulation (F1P2, 1% xanthan gum), the zeta potential values fluctuated within a narrow range (from −46.5 mV on day 1 to −50.6 mV at 40 °C by month 3). This uniformity throughout all the storage conditions verifies that the formulations maintained a strong negative surface charge, which helped preserve their physical integrity and nano-size distribution over time. Overall, the zeta potential results validate the assumption that the formulations maintained their electrostatic stability over the 3-month period, particularly noting that the increased xanthan gum content enhanced charge stabilisation.

The pH values of topical formulations are critical for evaluating their appropriateness for dermal application, as overly acidic or alkaline formulations may cause irritation or disturb the skin's natural acid mantle (Dalo et al., 2022). Throughout the three-month storage period, the pH values of all four NEG formulations consistently remained within a narrow and acceptable range, demonstrating good chemical stability under all three tested conditions. The initial pH values of the formulations were between 4.91 and 5.06, and after 3 months, they remained within the range of 4.54 to 5.04. Minor decreases were observed at elevated storage temperatures, especially at 40 ± 2 °C, aligning with the established impact of higher temperatures on hydrolytic degradation and slight changes in formulation equilibria. Nevertheless, no statistical or practical significance was found for these alterations.

All measured pH values fell within the physiologically acceptable range for topical applications (approximately pH 4.5–6.0), indicating that the formulations are unlikely to disrupt the skin's natural pH or cause irritation during use. The uniform pH stability observed in all samples and storage conditions indicates the robustness and skin compatibility of the developed NEG systems.

Measuring the electrical conductivity offers an emulsion system ionic strength insight into the aqueous phase's continuity (Ozkan et al., 2022). Across the four formulations of the NEG, the electrical conductivity was relatively constant throughout the three months of storage at all temperature conditions (5±3 °C, 25±2 °C / 60% RH, and 40±2 °C / 75% RH). These results confirm that the ionic environment and phase integrity of the formulations were well conserved over time. Initial conductivity values ranged from 480.0 to 631.5 µS, with minimal fluctuations observed at the conclusion of the 3-month period. F1P2 (1% xanthan gum) demonstrated a gradual and minor reduction in conductivity, decreasing from 575.5 µS

on day 1 to 542.0 µS at 25 °C by month 3, suggesting notable electrochemical stability.

The high conductivity values observed in all formulations are due to the aqueous continuous phase of the NEG systems. In oil-in-water (O/W) emulsions, water functions as the external phase, acting as the main medium for ion transport and consequently improving the overall conductivity (Kildaci et al., 2021). The presence of electrolytes and potentially dissociated functional groups from the gelling agents may have influenced the conductivity levels.

The slight fluctuation in the conductivity over time and varying temperature conditions demonstrates the physicochemical stability of the formulations, with no signs of phase inversion, ion depletion, or instability during storage.

The viscosity profiles of the four formulations (F1P2 1% XG, F1P2 1.5% XG, F3P1 1% XG, and F3P1 1.5% XG) were evaluated over a 3-month storage period under three different storage conditions. The results demonstrate that the viscosity values of the formulations remained stable throughout the 3-month storage period under all tested conditions (Figure 3), indicating the physical stability of the formulations over time. Furthermore, elevating the xanthan gum concentration from 1% to 1.5% resulted in a significant increase in the viscosity in both the F1P2 and F3P1 formulations (Figure 4-Figure 7). The findings indicate that xanthan gum significantly enhances the thickening and structural stability of the NEG matrix.

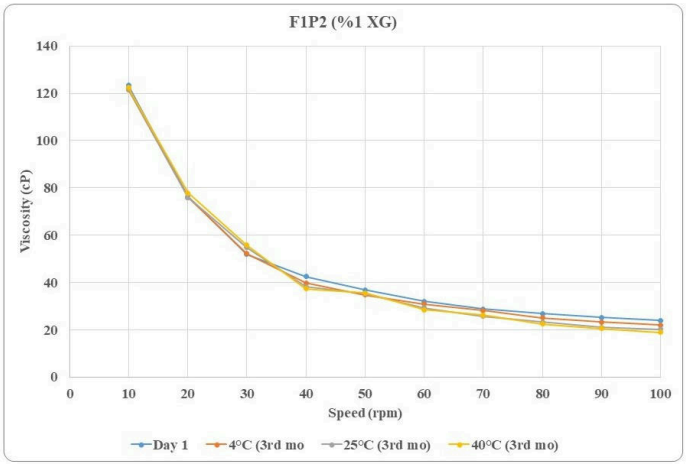

Figure 4. The viscosity values of F1P2 (%1 XG) NEGs, (means ± SD, n = 3). (Error bars were omitted for clarity)

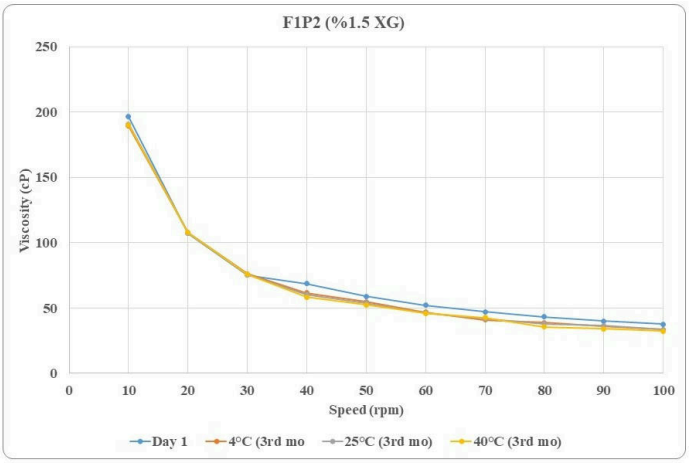

Figure 5. The viscosity values of F1P2 (%1.5 XG) NEGs, (means ± SD, n = 3). (Error bars were omitted for clarity)

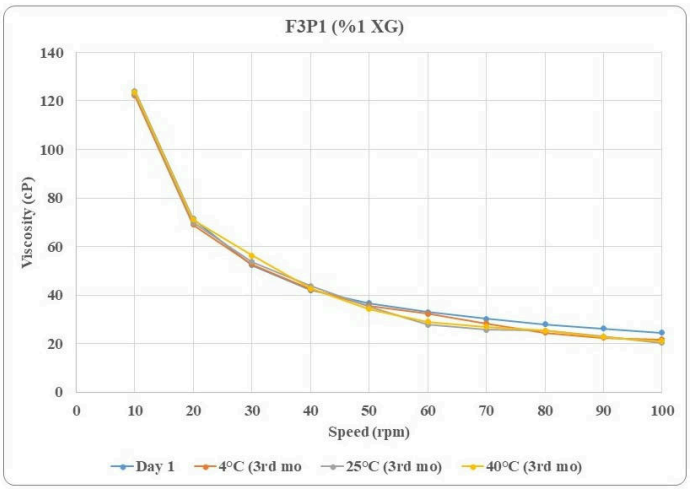

Figure 6. The viscosity values of F3P1 (%1 XG) NEGs, (means ± SD, n = 3). (Error bars were omitted for clarity)

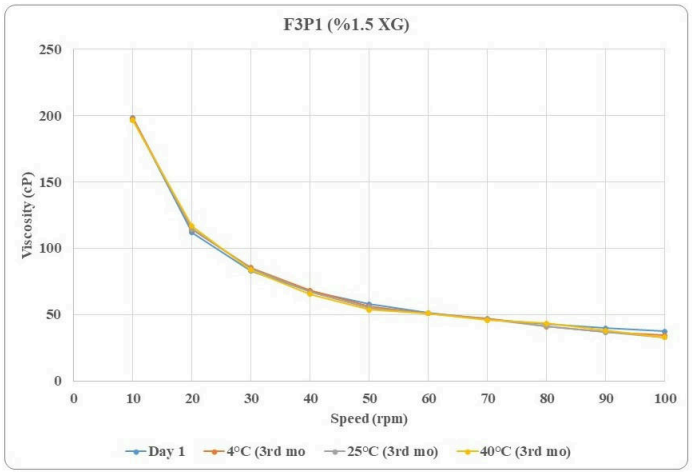

Figure 7. The viscosity values of F3P1 (%1.5 XG) NEGs, (means ± SD, n = 3). (Error bars were omitted for clarity)

The shear-thinning behaviour was observed in all of the formulations, meaning that the viscosity decreased as the shear rate (rpm) increased. This indicates a pseudoplastic flow type that is non-Newtonian, which is beneficial for topical applications (Calienni et al., 2023). This behaviour enables the product to spread easily upon application, due to the reduced viscosity under shear, while maintaining a stable structure during storage because of the increased viscosity at rest, thus ensuring both ease of application and product stability. The viscosity ranges that have been observed are suitable for dermal application, improving skin functionality and user comfort. The rheological properties and stability of the formulations indicate their potential as effective topical delivery systems in the NEG form.

In Vitro Cell Culture Studies

Cytotoxicity Test

The CCK-8 assay was used to evaluate the cytotoxic effects of the tested formulation (T: F1P2 %1 XG) and its placebo (P) on Vero cell cultures. The results were reported as cell inhibition percentages (%) for each of the serial dilutions (1/500 to 1/2000) (Table 3).

Table 3. Cell Inhibition Percentages (%) of Test and Placebo Nanoemulgel Formulations Across Serial Dilutions (1/500 to 1/2000)

Dilution Ratio	T (w/ Essential Oils) [% Inhibition]	P (Placebo) [% Inhibition]
1/500	94.50%	98.23%
1/750	82.26%	87.33%
1/1000	64.44%	71.02%
1/1500	59.02%	68.48%
1/1750	54.21%	59.26%
1/2000	52.92%	52.29%

Both the T and P formulations exhibited concentration-dependent cytotoxicity, as seen in the decreasing inhibition values with increasing dilution. This inverse correlation is expected and confirms the reliability of the CCK-8 assay in this context. At all concentrations, the formulation containing the essential oils demonstrated slightly lower inhibition values than the P. This finding supports that star anise and melissa essential oils did not increase cytotoxicity; in fact, their presence may have had a mildly protective or stabilising cellular effect.

T and P exhibited cytotoxicity at lower dilutions (1/500–1/1000). Cytotoxicity at dilutions of 1/1500 and higher was classified as borderline or mild, with no lethal effects visually detected, consistent with the established lethal dose (LD) range of 1/500 ≥ LD(n) > 1/1500. This indicates that the non-toxic threshold (LD) exceeded a 1/1500 dilution, aligning with the visual microscopic observations conducted during daily monitoring (Figure 8-Figure 10). No substance-induced CPE or cell death was observed at 1/1500 and 1/2000 dilutions. The half-maximal inhibitory concentration (IC_{50}) value, defined as the concentration at which 50% of the cells are inhibited, was estimated to be between 1/1750 and 1/2000 for both formulations. At a dilution of 1/2000, the inhibition values stabilised around 52%, indicating partial cytotoxicity that was not severe, even at increased dilutions.

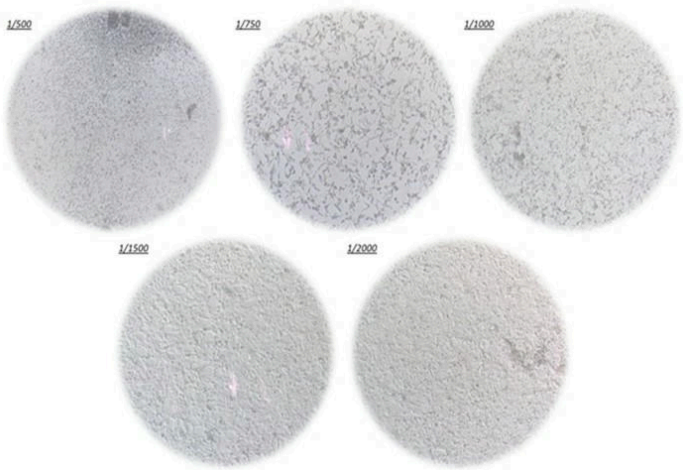

Figure 8. Microscope Images (Olympus IX71) of the test formulation showing the effects of different dilutions on Vero cells at 48 hours

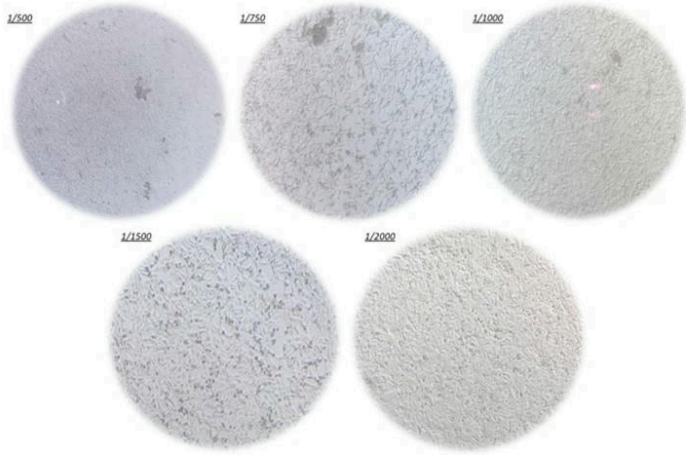

Figure 9. Microscope Images (Olympus IX71) of the placebo formulation showing the effects of different dilutions on Vero cells at 48 hours



Figure 10. Microscope Images (Olympus IX71) of the untreated control showing the effects of different dilutions on Vero cells at 48 hours

The findings demonstrate that the NEG incorporating star anise and melissa essential oils exhibits cytotoxicity levels comparable to the base formulation, confirming its safety at suitably diluted concentrations. This indicates the practicality of using these essential oils in topical applications, contingent upon adjusting the final applied concentrations to levels below the LD threshold.

Antiviral Activity Studies

The present study evaluated the antiviral activity of a NEG formulation (F1P2 %1 XG) incorporating the essential oils of *Melissa officinalis* (lemon balm) and *Illicium verum* (star anise) on HSV-1. Our results indicate that the T formulation viral titre in Vero cells was significantly less than the P formulation and untreated controls.

From the viral titration data, it could be seen that the test formulation had a 17.78-fold reduction in titre of HSV-1 ($1\times10^{4.5}$ $DKID_{50}$/mL) at 1/2000 dilution compared to the untreated virus control ($1\times10^{5.75}$ $DKID_{50}$/mL) (Table 4). The placebo formulation, with no essential oils, showed only a 1.77-fold reduction ($1\times10^{5.5}$ $DKID_{50}$/ml) compared with the control. This demonstrates that the antiviral action is likely due to the essential oils and not the NEG base components.

Table 4. Comparison of the HSV-1 viral load in Vero cells following treatment with the test formulation (T), placebo (P), and untreated control

Formulations and the HSV-1 Control Group	Viral Load ($DKID_{50}$/ mL)
T + HSV-1	$1x10^{4,5}$
P + HSV-1	$1x10^{5,5}$
Control	$1x10^{5,75}$

These results are in agreement with the literature where the essential oil of *Melissa officinalis* is documented to possess strong anti-HSV-1 activity. Studies have cited a more than 98.8% reduction in the plaque count at non-cytotoxic concentrations, probably due to citral and citronellal compounds that could block the viral binding and cell entry (Schnitzler et al., 2008). Moreover, encapsulated forms such as glycerosome-loaded lemon balm oil have shown greater stability and improved antiviral activity (Vanti et al., 2020).

Likewise, the essential oil of star anise is reported to have high antiviral activity against HSV-1 with an IC_{50} of 1 µg/mL and a selectivity index (SI) of 160. The major constituent of star anise oil, trans-anethole, is believed to interfere with cells and inhibit viral replication (Astani et al., 2011).

Supporting the development of the essential oil-based NEGs, the findings indicate that the gel containing essential oils from *Melissa officinalis* and *Illicium verum* not only demonstrates superior antiviral activity in comparison to the placebo but also proves to have reasonable cytocompatibility, thus reinforcing the possibility of employing these NEGs as efficient topical antiviral agents targeting HSV-1 infections.

Our antiviral studies demonstrated that the P formulation resulted in only a 1.77-fold reduction in HSV-1 titre compared with the untreated control, whereas the T formulation containing essential oils achieved a 17.78-fold reduction. The modest effect of the placebo can be explained by the known antiviral properties of *Quillaja saponaria* saponins, which are able to disrupt viral envelopes and reduce infectivity (Roner et al., 2007). Nevertheless, the dramatic difference between P and T confirms that the essential oils of *Melissa officinalis* and *Illicium verum* were the main contributors to the antiviral activity. This study design, comparing the essential oil-loaded NEG with its placebo base, ensured that the antiviral effect was correctly attributed to the essential oils while controlling for any background activity of the excipients.

Although a direct comparison with acyclovir was outside the boundaries of this study, literature reports have shown that the essential oils of *Melissa officinalis* and *Illicium verum* have strong anti-HSV-1 effects, sometimes equally or more effective than acyclovir in resistant strains. According to Astani et al. (2014), Melissa oil inhibited plaque formation in acyclovir-resistant HSV strains by over 98%, while *Illicium verum* oil showed a selectivity index of 160, which was higher than that typical for acyclovir (Astani et al., 2014). These findings, along with our noted 17.78-fold decrease in HSV-1 titer, demonstrate the potential of essential oil-based NEGs as potent topical antivirals, especially when cytocompatibility or resistance to synthetic agents restrict efficacy.

CONCLUSION

This research successfully developed and refined a biosurfactant-based NEG incorporating essential oils from *Melissa officinalis* and *Illicium verum* for topical use against HSV-1. The NEGs exhibited favourable physicochemical characteristics, sustained stability, and shear-thinning properties appropriate for dermal use. Cytotoxicity studies demonstrated the safety of the test formulation at suitable dilutions, while antiviral assays indicated a notable decrease in the HSV-1 viral titre, which is ascribed to the antiviral properties of the essential oils. The findings indicate that the developed NEG is a viable candidate for subsequent clinical evaluation as a topical therapeutic agent for HSV infections.

Peer Review Externally peer-reviewed.
Author Contributions Conception/Design of Study-.E.A.; Data Acquisition-.E.A., T.K., Z.O., M.Y., S.P.; Data Analysis/Interpretation- E.A., H.S.P., M.A., S.Y..; Drafting Manuscript- E.A..; Critical Revision of Manuscript-E.A., S.P..; Final Approval and Accountability- T.K., E.A., T.K., Z.O., M.Y., H.S.P., M.A., S.Y.
Conflict of Interest The authors have no conflict of interest to declare.
Grant Support The present work was supported by the Research Fund of İstanbul University. Project No: 39717.

Author Details

Tuğba Kaman
[1] İstanbul University, Graduate School of Health Sciences, İstanbul, Türkiye
[2] Üsküdar University, Vocational School of Health Services, Medical and Aromatic Plants, İstanbul, Türkiye
0000-0002-5885-0193

Ebru Altuntaş
[3] İstanbul University, Faculty of Pharmacy, Department of Pharmaceutical Technology, Istanbul, Türkiye
0000-0003-2902-5554 ebru.altuntas@istanbul.edu.tr

Zakaria Ouzaid
[1] İstanbul University, Graduate School of Health Sciences, İstanbul, Türkiye
[3] İstanbul University, Faculty of Pharmacy, Department of Pharmaceutical Technology, Istanbul, Türkiye
0009-0003-1160-853X

Merve Yılmaz
[3] İstanbul University, Faculty of Pharmacy, Department of Pharmaceutical Technology, Istanbul, Türkiye
0009-0006-0708-1992

Hasan Sercan Palancı
[4] Selcuk University, Department of Virology, Faculty of Veterinary Medicine, Konya, Türkiye
0000-0001-5408-9176

Mustafa Altındiş
[5] Sakarya University, Department of Basic Medical Sciences, School of Medicine, Sakarya, Türkiye
0000-0003-0411-9669

Sibel Yavru
[4] Selcuk University, Department of Virology, Faculty of Veterinary Medicine, Konya, Türkiye
0000-0002-5839-364X

REFERENCES

Allahverdiyev, A., Duran, N., Ozguven, M., & Koltas, S. (2004). Antiviral activity of the volatile oils of *Melissa officinalis* L. against *Herpes simplex* virus type-2. *Phytomedicine*, *11*(7-8), 657-661.

Altuntaş, E., & Yener, G. (2017). Formulation and evaluation of thermoreversible in situ nasal gels containing mometasone furoate for allergic rhinitis. *AAPS PharmSciTech*, *18*, 2673-2682.

Aman, R. M., Abu Hashim, I. I., & Meshali, M. M. (2020). Novel Clove essential oil nanoemulgel tailored by Taguchi's model and scaffold-based nanofibers: Phytopharmaceuticals with promising potential as cyclooxygenase-2 inhibitors in external inflammation. *International Journal of Nanomedicine*, 2171-2195.

Astani, A., Heidary Navid, M., & Schnitzler, P. (2014). Attachment and penetration of Acyclovir-resistant herpes simplex virus are inhibited by melissa officinalis extract. *Phytotherapy Research*, *28*(10), 1547-1552.

Astani, A., Reichling, J., & Schnitzler, P. (2011). Screening for antiviral activities of isolated compounds from essential oils. *Evidence-Based Complementary and Alternative Medicine*, *2011*(1), 253643.

Astani, A., Reichling, J., & Schnitzler, P. (2012). *Melissa officinalis* extract inhibits attachment of herpes simplex virus *in vitro*. *Chemotherapy*, *58*(1), 70-77.

Banerjee, A., Binder, J., Salama, R., & Trant, J. F. (2021). Synthesis, characterization and stress-testing of a robust quillaja saponin stabilized oil-in-water phytocannabinoid nanoemulsion. *Journal of Cannabis Research*, *3*, 1-14.

Belgheisi, S., Motamedzadegan, A., Milani, J. M., Rashidi, L., & Rafe, A. (2021). Impact of ultrasound processing parameters on physical characteristics of lycopene emulsion. *Journal of Food Science and Technology*, *58*(2), 484-493.

Calienni, M. N., Martínez, L. M., Izquierdo, M. C., Alonso, S. d. V., & Montanari, J. (2023). Rheological and viscoelastic analysis of hybrid formulations for topical application. *Pharmaceutics*, *15*(10), 2392.

Carpenter, J., & Saharan, V. K. (2017). Ultrasonic assisted formation and stability of mustard oil in water nanoemulsion: Effect of process parameters and their optimization. *Ultrasonics Sonochemistry*, *35*, 422-430.

Dalo, F., Yener, F. G., Altuntaş, E., & Döşler, S. (2022). A Cosmetic Nanoemulsion Against Seborrheic Dermatitis: Development, Characterization and Effectiveness. *Fabad Journal of Pharmaceutical Sciences*, *47*(2), 213-230.

Demir, T., & Akpinar, Ö. (2021). Fitokimyasalların Antiviral Etkileri. *Düzce Üniversitesi Bilim ve Teknoloji Dergisi*, *9*(4), 1519-1535.

Doost, A. S., Van Camp, J., Dewettinck, K., & Van der Meeren, P. (2019). Production of thymol nanoemulsions stabilized using Quillaja Saponin as a biosurfactant: Antioxidant activity enhancement. *Food Chemistry*, *293*, 134-143.

Frey, H.-R., & Liess, B. (1971). Growth curve studies and applicability of a highly cytopathogenic BVD-MD-virus strain for diagnostic purposes using the microtitre method.

Gaikwad, S. G., & Pandit, A. B. (2008). Ultrasound emulsification: effect of ultrasonic and physicochemical properties on dispersed phase volume and droplet size. *Ultrasonics Sonochemistry*, *15*(4), 554-563.

Jiang, Y.-C., Feng, H., Lin, Y.-C., & Guo, X.-R. (2016). New strategies against drug resistance to herpes simplex virus. *International Journal of Oral Science*, *8*(1), 1-6.

Kaur, K., Kumar, R., & Mehta, S. (2016). Formulation of saponin stabilized nanoemulsion by ultrasonic method and its role to protect the degradation of quercitin from UV light. *Ultrasonics Sonochemistry*, *31*, 29-38.

KC, S., Kakoty, V., Krishna, K. V., Dubey, S. K., Chitkara, D., & Taliyan, R. (2021). Neuroprotective efficacy of co-encapsulated rosiglitazone and vorinostat nanoparticle on streptozotocin induced mice model of Alzheimer disease. *ACS Chemical Neuroscience*, *12*(9), 1528-1541.

Kildaci, I., Budama-Kilinc, Y., Kecel-Gunduz, S., & Altuntas, E. (2021). Linseed Oil Nanoemulsions for treatment of Atopic Dermatitis disease: Formulation, characterization, *in vitro* and *in silico* evaluations. *Journal of Drug Delivery Science and Technology*, *64*, 102652.

Leong, T., Wooster, T., Kentish, S., & Ashokkumar, M. (2009). Minimising oil droplet size using ultrasonic emulsification. *Ultrasonics Sonochemistry*, *16*(6), 721-727.

Leung, A. K., & Barankin, B. (2017). Herpes labialis: an update. *Recent Patents on Inflammation & Allergy Drug Discovery*, *11*(2), 107-113.

Mulia, K., Ramadhan, R. M., & Krisanti, E. A. (2018). Formulation and characterization of nanoemulgel mangosteen extract in virgin coconut oil for topical formulation. MATEC Web of Conferences,

Nafisi, S., & Maibach, H. (2017). Nanotechnology in cosmetics. *Cosmetic Science and Technology: Theoretical Principles and Applications; Elsevier: Amsterdam, The Netherlands*, *337*.

Nastiti, C. M., Ponto, T., Abd, E., Grice, J. E., Benson, H. A., & Roberts, M. S. (2017). Topical nano and microemulsions for skin delivery. *Pharmaceutics*, *9*(4), 37.

Nirmala, M. J., Durai, L., Rao, K. A., & Nagarajan, R. (2020). Ultrasonic nanoemulsification of Cuminum cyminum essential oil and its applications in medicine. *International Journal of Nanomedicine*, 795-807.

Ozkan, B., Altuntas, E., Cakir Koc, R., & Budama-Kilinc, Y. (2022). Development of piperine nanoemulsions: an alternative topical application for hypopigmentation. *Drug Development and Industrial Pharmacy*, *48*(3), 117-127.

Pandi, P., Jain, A., Kommineni, N., Ionov, M., Bryszewska, M., & Khan, W. (2018). Dendrimer as a new potential carrier for topical delivery of siRNA: A comparative study of dendriplex vs. lipoplex for delivery of TNF-α siRNA. *International Journal of Pharmaceutics*, *550*(1-2), 240-250.

Roner, M. R., Sprayberry, J., Spinks, M., & Dhanji, S. (2007). Antiviral activity obtained from aqueous extracts of the Chilean soapbark tree (Quillaja saponaria Molina). *Journal of General Virology*, *88*(1), 275-285.

Saka, R., Jain, H., Kommineni, N., Chella, N., & Khan, W. (2020). Enhanced penetration and improved therapeutic efficacy of bexarotene via topical liposomal gel in imiquimod induced psoriatic plaque model in BALB/c mice. *Journal of Drug Delivery Science and Technology*, *58*, 101691.

Sarkhel, S. (2016). Evaluation of the anti-inflammatory activities of Quillaja saponaria Mol. saponin extract in mice. *Toxicology Reports*, *3*, 1-3.

Schnitzler, P., Schön, K., & Reichling, J. (2001). Antiviral activity of Australian tea tree oil and eucalyptus oil against herpes simplex virus in cell culture. *Die Pharmazie*, *56*(4), 343-347.

Schnitzler, P., Schuhmacher, A., Astani, A., & Reichling, J. (2008). Melissa officinalis oil affects infectivity of enveloped herpesviruses. *Phytomedicine*, *15*(9), 734-740.

Schreiner, T. B., Santamaria-Echart, A., Ribeiro, A., Peres, A. M., Dias, M. M., Pinho, S. P., & Barreiro, M. F. (2020). Formulation and optimization of nanoemulsions using the natural surfactant saponin from quillaja bark. *Molecules*, *25*(7), 1538.

Shukla, T., Upmanyu, N., Agrawal, M., Saraf, S., Saraf, S., & Alexander, A. (2018). Biomedical applications of microemulsion through dermal and transdermal route. *Biomedicine & Pharmacotherapy*, *108*, 1477-1494.

Sivesind, T., Viola, J., Zhang, L., Dellavalle, R., & Chi, C.-C. (2022). From the Cochrane Library: Interventions for the Prevention of Herpes Simplex Labialis (Cold Sores on the Lips). *JMIR Dermatology*, *5*(2), e38322.

Szumała, P., & Macierzanka, A. (2022). Topical delivery of pharmaceutical and cosmetic macromolecules using microemulsion systems. *International Journal of Pharmaceutics*, *615*, 121488.

van de Sand, L., Bormann, M., Schmitz, Y., Heilingloh, C. S., Witzke, O., & Krawczyk, A. (2021). Antiviral active compounds derived from natural sources against herpes simplex viruses. *Viruses*, *13*(7), 1386.

Vanti, G., Ntallis, S. G., Panagiotidis, C. A., Dourdouni, V., Patsoura, C., Bergonzi, M. C., Lazari, D., & Bilia, A. R. (2020). Glycerosome of Melissa officinalis L. essential oil for effective anti-HSV Type 1. *Molecules*, *25*(14), 3111.

Yang, Y., Leser, M. E., Sher, A. A., & McClements, D. J. (2013). Formation and stability of emulsions using a natural small molecule surfactant: Quillaja saponin (Q-Naturale®). *Food Hydrocolloids*, *30*(2), 589-596.

Yap, X. F., Saw, S. H., Lim, V., & Tan, C. X. (2024). Plant essential oil nanoemulgel as a cosmeceutical ingredient: A review. *Cosmetics*, *11*(4), 116.

Zhang, K., Lv, D.-W., & Li, R. (2019). Conserved herpesvirus protein kinases target SAMHD1 to facilitate virus replication. *Cell Reports*, *28*(2), 449-459. e445.